Monatshefte für Chemie 138, 1217–1223 (2007)
DOI 10.1007/s00706-007-0725-z
Printed in The Netherlands

Monatshefte für Chemie
Chemical Monthly

A Theoretical Study of Amine Bonding in Titanium Alkoxide Adducts

Maurizio Casarin[1,*], **Andrea Vittadini**[2], and **Ulrich Schubert**[3]

[1] Dipartimento di Scienze Chimiche, Università di Padova, Padova, Italy
[2] Istituto di Scienze e Tecnologie Molecolari del CNR, Padova, Italy
[3] Institute of Materials Chemistry, Vienna University of Technology, Wien, Austria

Received April 25, 2007; accepted May 21, 2007; published online September 24, 2007

Summary. DFT calculations were carried out on $Ti_2(OCH_3)_8(NH_2CH_3)_2$ and $Ti_2(OCH_3)_8(NH_3)_2$, which are model compounds for the previously isolated amine adducts $Ti_2(OR)_8(NH_2R')_2$. The calculations show that the Ti–N bond strength is weak; however, coordination of the amine to the metal center is supported by a N–H···O hydrogen bond of the amine with the neighboring alkoxo ligand. The Ti–N interaction is purely σ in nature, while the Ti–O interactions include both σ and π contributions. The lowest unoccupied molecular orbitals are mainly localized on Ti t_{2g}-like orbitals.

Keywords. Density functional calculations; Coordination chemistry; Transition metal compounds; Titanium alkoxides; Amine adducts.

Introduction

Group IVB alkoxides, $M(OR)_4$ (M = Ti, Zr, Hf), are important compounds for catalysis, chemical vapor deposition, or sol–gel processes [1]. Their chemical properties are, to a high degree, determined by the *Lewis* acidity of the metal atom. Donor–acceptor interactions with alkoxo groups of other $M(OR)_4$ entities, resulting in alkoxo-bridged oligomers $[M(OR)_4]_n$, and interaction with *Lewis* basic co-reactants, additives, or solvent molecules, especially alcohols, are the most important cases to be considered in sol–gel systems. The coordination number of the metal is increased by the donor–acceptor interaction.

We recently investigated the interaction of amines with $Ti(OR)_4$ in more detail and characterized the adducts $Ti_2(OR)_8(NH_2R')_2$ in solution and in the crystalline state [2–4]. The dimeric adducts are formed when $Ti(OR)_4$ is reacted with primary amines, $R'NH_2$ (Eq. (1)).

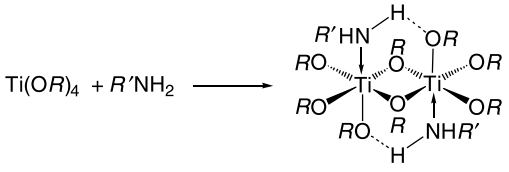

(1)

The metal atoms in the adducts are octahedrally coordinated owing to both the formation of alkoxo bridges and coordination of the amine molecule. The latter is additionally hydrogen-bonded to a neighboring alkoxo ligand. This turned out to be very important with regard to the stability of the adducts. In a series of amine adducts $M_2(O^iPr)_8(NH_2R)_2$ (M = Ti, Zr), stability of the adducts not only depended on the basicity of the amine but to a large extent also on the hydrogen-donor ability of the amine [4]. Thus, secondary amines R_2NH resulted in less stable adducts; although they are more basic than primary amines, they are weaker hydrogen donors in NH···O bonds.

The general structural motif of the adducts $Ti_2(OR)_8(NH_2R')_2$ is retained in coordination polymers, $Ti_2(OR)_8[NH_2–X–NH_2]$, formed from $Ti(OR)_4$ and diamines [2, 3], as well as in aminoalcoholate derivatives $Ti_2(OR)_6(OCH_2CH_2NH_2)_2$ [5].

* Corresponding author. E-mail: maurizio.casarin@unipd.it

To gain a deeper understanding of the interaction of amines (as model *Lewis* bases) with titanium alkoxides, quantum mechanical calculations were carried out on $Ti_2(OMe)_8(NH_2Me)_2$ ($\mathbf{M^1}$). $\mathbf{M^1}$ is a model of $Ti_2(OR)_8(NH_2R')_2$, where the groups R and R' were replaced by methyl groups. The outcome of these calculations is reported in this article.

Computational Details

Calculations [6] were carried out at the Laboratorio Interdipartimentale di Chimica Computazionale (LICC) of the University of Padova. Optimized geometries (extended to all atoms outside the equatorial Ti_2O_6 plane), vibrational parameters and excitation energies were obtained by employing generalized gradient (GGA) corrections self-consistently included through the *Becke–Perdew* (*BP*) formula [7]. Force constants and harmonic frequencies were calculated by numerical differentiation of energy gradients both at the equilibrium geometry (C_i symmetry point group) and at slightly deviating geometries. Triple-ζ *Slater*-type basis sets were adopted for the Ti atoms and the atoms directly bonded to Ti, as well as for the N–H atoms of the amine ligands. A double-ζ basis set was employed for the remaining atoms. Inner cores of Ti (1s2s2p), O (1s), C (1s), and N (1s) atoms were kept frozen throughout the calculations.

The binding energy (*BE*) was analyzed in terms of fragment orbitals by applying the *Ziegler*'s extended transition state method (ETS) [8]. According to the ETS method, $BE = \Delta E_{es} + \Delta E_{Pauli} + \Delta E_{int} + \Delta E_{prep}$, where ΔE_{es} is the pure electrostatic interaction, ΔE_{Pauli} is the destabilizing two-orbital-four-electron interaction between the occupied orbitals of the interacting fragments, ΔE_{int} derives from the stabilizing interaction between occupied and empty orbitals of the interacting fragments, and ΔE_{prep} provides information about the energy required to relax the structure of the free fragments to the geometry they assume in the final system.

Instead of displaying discrete eigenvalues along an energy axis, we preferred to plot the density of states (hereafter DOS) as a function of energy by using a 0.25 eV Lorentzian broadening factor. These plots, based on *Mulliken*'s prescription for partitioning the overlap density [9], have the advantage of providing insights into the atomic composition of MOs over a broad range of energy. Partial density of states (PDOS) is

$$\mathrm{PDOS}^{\nu}_{nl}(\varepsilon) = \sum_p f^{\nu}_{nl,p} \frac{\gamma/\pi}{(\varepsilon - \varepsilon_p)^2 + \gamma^2}$$

while

$$\mathrm{DOS}(\varepsilon) = \sum_{\nu,n,l} \mathrm{PDOS}^{\nu}_{nl}(\varepsilon) = \sum_p \frac{g_p \gamma/\pi}{(\varepsilon - \varepsilon_p)^2 + \gamma^2}$$

where $f^{\nu}_{nl,p}$ is the *Mulliken*'s population contribution from atom ν, state (nl) to the pth MO of energy ε_p and degeneracy g_p. Crystal orbital overlap population (COOP) [10] curves were obtained by weighting one-electron energy levels by their basis orbital percentage to obtain information about the localization and the bonding/antibonding character of selected MOs. Finally, lowest lying excitation energies and corresponding oscillator strengths were evaluated by employing the time dependent DFT (TDDFT) approach [11]. The level of theory exploited for TDDFT calculations was the same used in previous numerical experiments.

Results and Discussion

The crystallographically determined centrosymmetric structure of $Ti_2(O^iPr)_8(NH_2Pr)_2$ (**1**) [2] was taken as a starting point for the calculations. Each Ti atom of **1** is octahedrally coordinated by the oxygen atoms of five alkoxo groups (hereafter labeled O_a, O_b, and O_e, corresponding to O_{apical}, $O_{bridging}$, and $O_{equatorial}$) as well as to the nitrogen atom of an amine, with the two distorted octahedra sharing a common edge. Both the long Ti–N bond distance (2.311(2) Å) and the chemical behavior of the dimer (being not very stable under reduced pressure) are consistent with a rather weak Ti–N interaction. Crystallographic results also indicated a quite strong $O_a\cdots HN$ hydrogen bonding as testified by the significant bending of the primary amine towards the neighboring axial alkoxo ligand (the N–Ti–O_b bond angle is about 80°), the rather short $O_a\cdots N$ internuclear distance (2.952(2) Å), and the wide N–H$\cdots O_a$ angle (160°).

A series of DFT calculations was carried out on $Ti_2(OCH_3)_8(NH_2CH_3)_2$ ($\mathbf{M^1}$) as a model of **1**. All calculations were run by imposing a C_i symmetry, as found in the solid-state structure of **1**. Inspection of Fig. 1, where selected optimized geometrical parameters of $\mathbf{M^1}$ are reported, reveals that computed

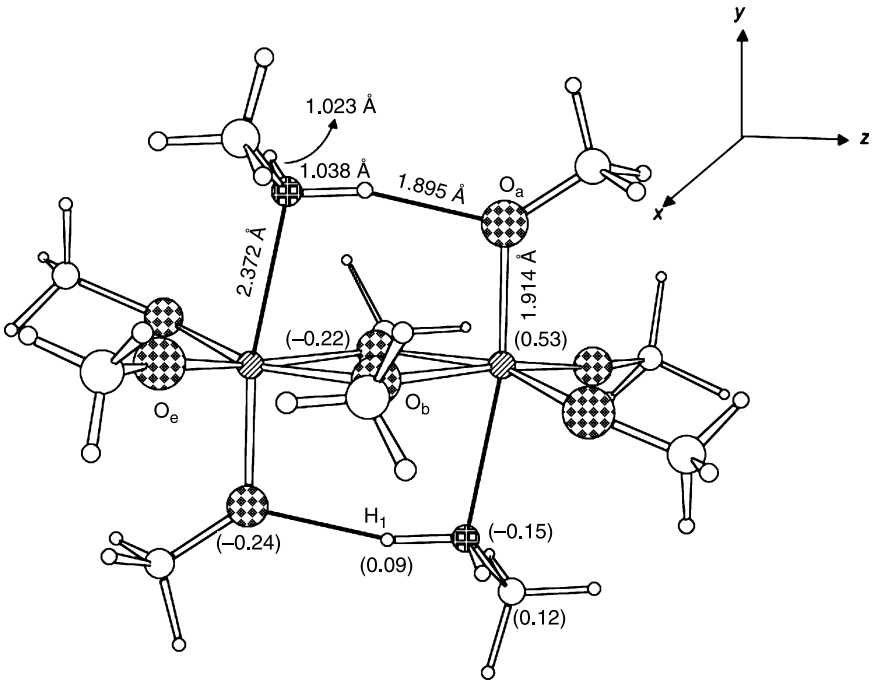

Fig. 1. Selected optimized geometrical parameters of $Ti_2(OMe)_8(NH_2Me)_2$ (**M**[1]). Selected gross atomic charges (in parentheses) are also reported. Ti–N–C 120.7, Ti–N–H_2 104.6, Ti–N–H_1 103.5, N–H_1–O 165.0, N–Ti–O_b 80.6°. Bending angle of $MeNH_2$ ligand 12.3°. $\nu_{N\text{-}H1}$ 3171, $\nu_{N\text{-}H2}$ 3427 cm^{-1}

quantities agree very well with the crystallographically determined values of **1**. In particular, the optimized N–Ti–O_b and N–H···O_a angles (80.6 and 165.0°) well reproduce the corresponding angles of **1**. The rather long N–H bond distance (1.038 Å) induced by the hydrogen bonding also has to be noticed. According to that, the computed N–H stretching frequency (ν_{NH}) is significantly different for the H atoms of the primary amine, *viz.* 3171 *vs.* 3427 cm^{-1}.

The hydrogen bonding strength was estimated in another series of calculations. To this end, another model of **1** was considered, *viz.* $Ti_2(OCH_3)_8(NH_3)_2$

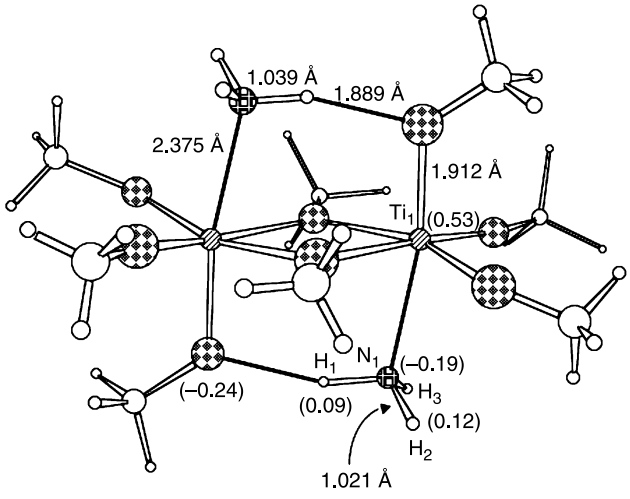

Fig. 2. Selected optimized geometrical parameters of $Ti_2(OMe)_8(NH_3)_2$ (**M**[2]) starting with a geometry similar to that of **M**[1]. Ti–N_1–H_3 112.9, Ti–N_1–H_2 114.0, Ti–N_1–H_1 105.5, N–H_1–O 162.2, N–Ti–O_b 78.5°. Bending angle of NH_3 ligand 12.5°. Bonding energy 6232.68 kJ · mol^{-1}

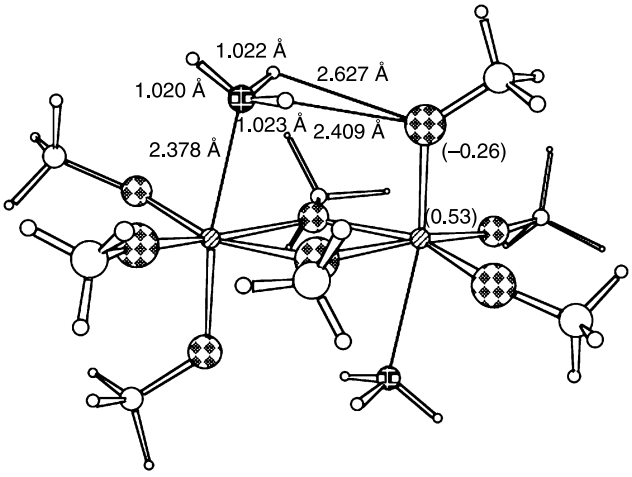

Fig. 3. Selected optimized geometrical parameters of $Ti_2(OMe)_8(NH_3)_2$ (**M**[2]) starting with an N–Ti–O_b angle of 90° and the NH atoms twisted away of O_a. Bonding energy 6228.00 kJ · mol^{-1}

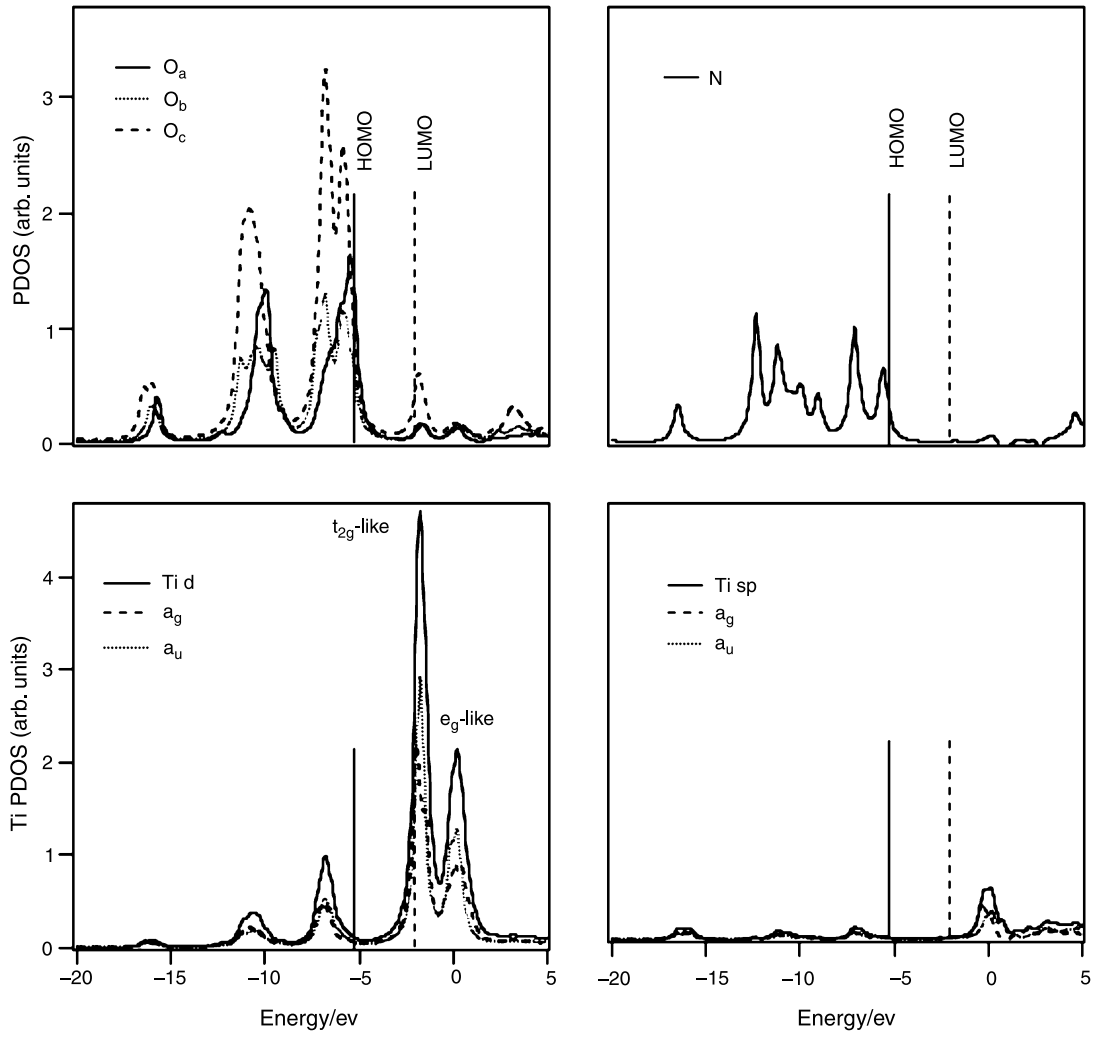

Fig. 4. M^1 partial density of states (PDOS) of O, N, and Ti. Vertical bars correspond to the HOMO and LUMO energies

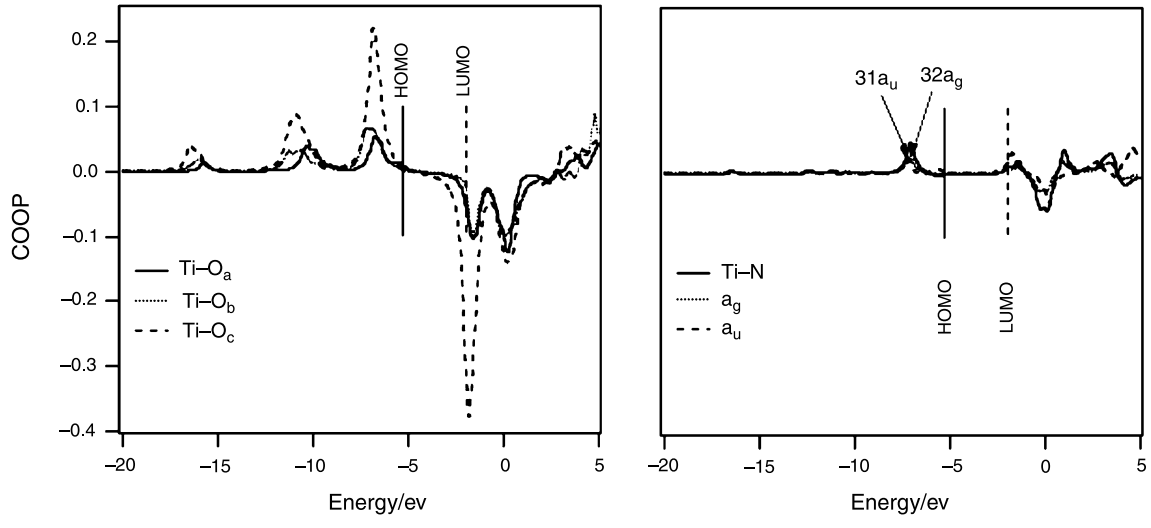

Fig. 5. M^1 COOP curves. Bonding and antibonding states correspond to positive and negative COOPs, respectively

($\mathbf{M^2}$), where the primary amine ligands were substituted by ammonia molecules. The first calculation on $\mathbf{M^2}$ was done by optimizing the geometrical parameters of the ligands out of the equatorial plane. A starting geometry for the NH_3 molecules was assumed similar to that of methylamine in $\mathbf{M^1}$. Comparison of geometrical parameters and *Hirshfeld* charges [12, 13] reported in Figs. 1 and 2 confirms the negligible effect induced by the substitution of the alkyl groups with hydrogen atoms. The second set of calculations on $\mathbf{M^2}$ was run with a different starting geometry. The starting N–Ti–O_b angle was set to 90°, and the hydrogen atoms of the ammonia ligand were positioned as far away from O_a as possible. Interestingly, the optimized parameters once again indicate a significant bending of NH_3 toward O_a (N–Ti–$O_b = 79.6°$) despite a different distance between O_a and the ammonia hydrogen atoms pointing toward it (Fig. 3). The latter is another local minimum in the potential energy hypersurface. As a whole, these results prevent the possibility of obtaining an estimate of the hydrogen-bonding strength in $\mathbf{M^1}$.

Further calculations were then carried out for the $Ti_2(OCH_3)_8$ and NH_2CH_3 fragments in $\mathbf{M^1}$ in order to evaluate the Ti–N bond strength. Binding energy (*BE*) calculations for $Ti_2(OCH_3)_8$ were done by assuming either the optimized geometry of $\mathbf{M^1}$ ($22224\,kJ \cdot mol^{-1}$) or by optimizing the coordinates of the apical methoxy groups ($5309.85\,kJ \cdot mol^{-1}$). Analogous considerations hold for calculations carried out for the free NH_2CH_3 (3375 and $3376\,kJ \cdot mol^{-1}$). The ΔBE between the binding energy computed by optimizing geometrical parameters in the free fragment and that obtained by using the optimized parameters of $Ti_2(OCH_3)_8$ in $\mathbf{M^1}$ is known as preparation energy. If BE_1 is the binding energy of $\mathbf{M^1}$ ($29135\,kJ \cdot mol^{-1}$), and BE_2 and BE_3 those of the optimized $Ti_2(OCH_3)_8$ and NH_2CH_3 "free" fragments, the Ti–N *BE* corresponds to $(BE_1 - BE_2 - 2BE_3)/2$. The computed value is $18\,kJ \cdot mol^{-1}$, thus confirming the weakness of the interaction.

Moving to the analysis of the electronic structure of $\mathbf{M^1}$, the first thing to be noticed is that the crystal field experienced by the Ti atoms lifts the degeneracy of their empty 3d AOs, giving rise to t_{2g}- and e_g-like components which, in C_i symmetry, result in symmetric (a_g) and anti-symmetric (a_u) combinations (see the Ti PDOS in Fig. 4). The highest occupied molecular orbitals (HOMOs) correspond to the $36a_g$–$39a_g$ and $36a_u$–$39a_u$ orbitals, for a total of eight levels all localized on the O/N 2p atomic orbitals, with non-bonding character with respect to the Ti–O and Ti–N interactions and spanning a quite narrow energy range (0.7 eV).

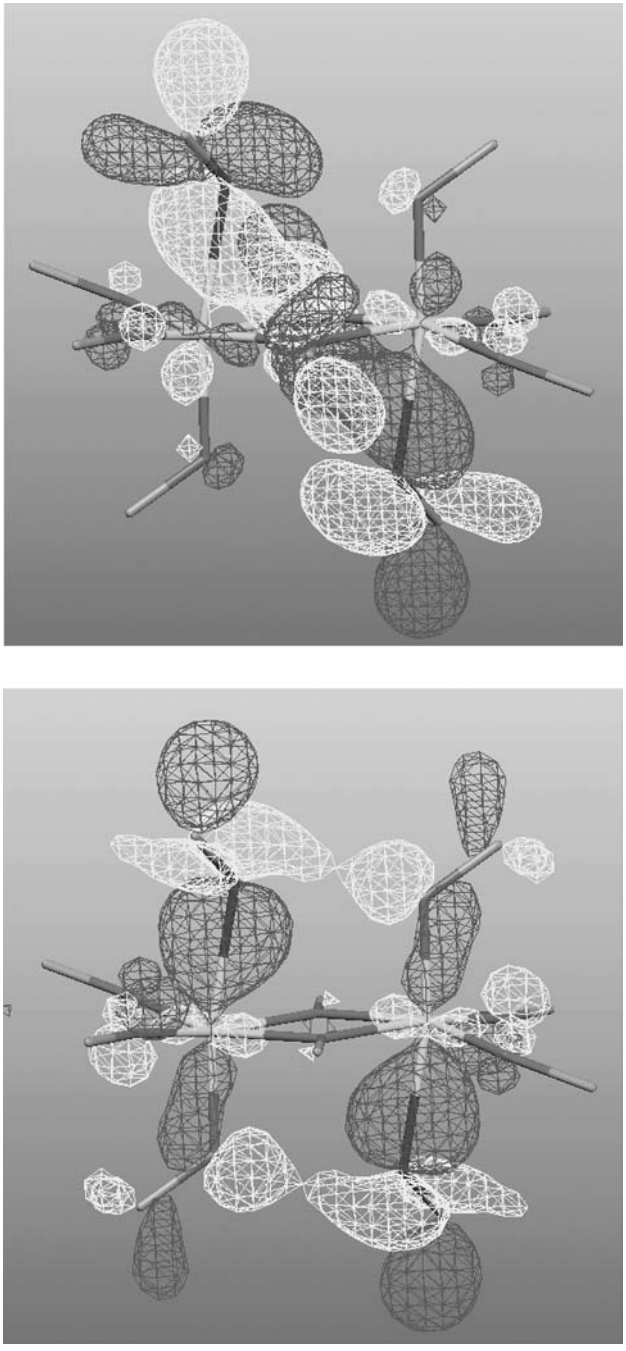

Fig. 6. 3D contour plots of the $31a_u$ (top) and $32a_g$ (bottom) MOs. Dark and light surfaces correspond to the wave function values of $0.03\,e^{1/2}/Å^{3/2}$ and $-0.03\,e^{1/2}/Å^{3/2}$

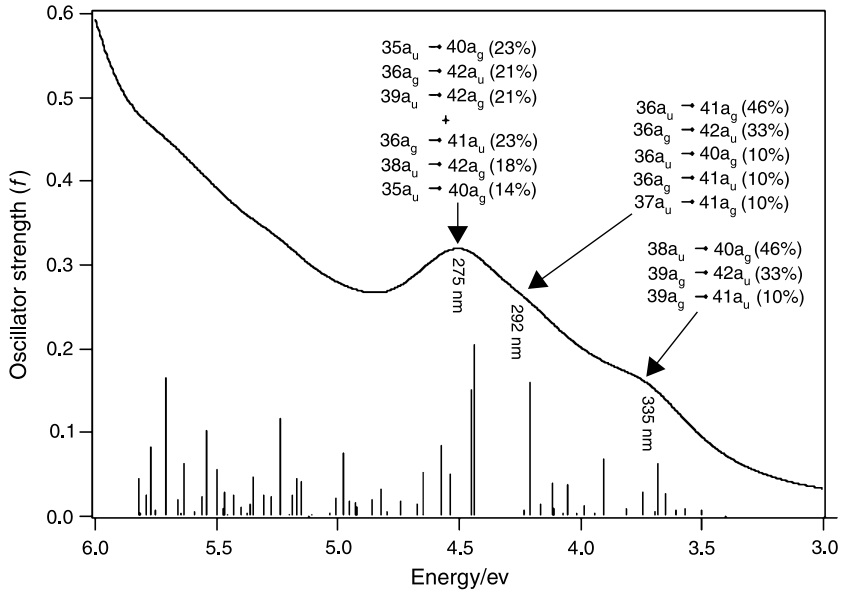

Fig. 7. TD-DFT excitation spectra of $\mathbf{M^1}$. The convoluted profile was obtained with a Lorentzian broadening of 0.25 eV. Only, lowest lying singlet–singlet transitions are reported

As pointed out before, COOP curves were computed to get information about the localization and the bonding/antibonding character of selected MOs. Inspection of Fig. 5 shows that (i) bonding partners lie at lower energies than the HOMOs, (ii) Ti–O interactions include both σ and π contributions, where the σ contribution is at ≈ -10 eV and the π contribution at ≈ -7 eV, and (iii) the Ti–N bonding is significantly weaker than that of Ti–O (in fact, the Ti–N bonding interaction is the weakest among those reported in the figure) and only σ in nature. Moreover, the $31a_u$ and $32a_g$ MOs, accounting for the Ti–N σ bonding (Fig. 6), lie in the same energy region (≈ -7 eV) as the Ti–O π bonding MOs.

The lowest unoccupied molecular orbitals (LUMOs) correspond to (i) the symmetric ($40a_g$–$42a_g$) and antisymmetric ($40a_u$–$42a_u$) combinations of Ti based t_{2g}-like orbitals, and (ii) the antibonding partners of the Ti–O π interaction (see Fig. 5). Interestingly, the simulated spectrum in the UV-Vis energy range is characterized by three spectral features: one band at 4.47 eV and two evident shoulders on its lower energy side (at 4.25 and 3.73 eV). Data reported in Fig. 7 clearly indicate that all these features correspond to excitations deriving from a strong mixing of configurations mainly characterized by HOMOs → LUMOs excited configurations.

Conclusions

The DFT calculations carried out on the model compounds $Ti_2(OCH_3)_8(NH_2CH_3)_2$ ($\mathbf{M^1}$) and $Ti_2(OCH_3)_8(NH_3)_2$ ($\mathbf{M^2}$) substantiate the conclusions drawn from the chemical behavior and the solid-state structures of various $Ti_2(OR)_8(NH_2R')_2$ compounds. The Ti–N bond is relatively weak (75 kJ/mol) and would not account for the stability of the amine adducts. However, the interaction is supported by a N–H···O_a hydrogen bond. Although it was not possible to quantify the strength of this interaction, geometry optimizations of both $\mathbf{M^1}$ and $\mathbf{M^2}$ clearly show that the amine bends towards O_a. This distortion can only be explained by assuming a rather strong hydrogen-bonding interaction.

The electronic structure of $\mathbf{M^1}$ is characterized by the HOMOs localized on 2p atomic orbitals of O and N atoms and being non-bonding with regard to Ti–O and Ti–N. The LUMOs are mainly localized on t_{2g}-like MOs and account for the antibonding part of the Ti–O π interactions. Ti–O interactions include both σ and π contributions, while the nature of the Ti–N interaction is purely σ, the Ti–N bonding being significantly weaker than that of Ti–O.

Acknowledgements

The work of *U.S.* was supported by the Fonds zur Förderung der wissenschaftlichen Forschung (FWF), Wien. The Labora-

torio Interdipartimentale di Chimica Computazionale (LICC) dell'Università di Padova is acknowledged for support of the computer facilities.

References

[1] Review articles: (a) Schubert U (2005) J Mater Chem **15**: 3701; (b) Schubert U (in press) Acc Chem Res
[2] (a) Fric H, Schubert U (2005) New J Chem **29**: 232; (b) Schubert U, Bauer U, Fric H, Puchberger M, Rupp W, Torma V (2005) Mat Res Soc Symp Proc **847**: 533
[3] Fric H, Puchberger M, Schubert U (2007) Eur J Inorg Chem 376
[4] Fric H, Puchberger M, Schubert U (2006) J Sol-Gel Sci Technol **40**: 155
[5] Fric H, Kogler FR, Puchberger M, Schubert U (2004) Z Naturforsch B **59**: 1241
[6] Amsterdam Density Functional Package, Version 2005, Vrjie Universiteit, Amsterdam, Netherlands
[7] (a) Becke AD (1988) Phys Rev A **38**: 3098; (b) Perdew JP (1986) Phys Rev B **33**: 8822
[8] Ziegler T, Rauk A (1977) Theor Chim Acta **46**: 1
[9] Mulliken RS (1955) J Chem Phys **23**: 1833
[10] Hoffmann R (1988) Solids and Surfaces: A Chemist's View of Bonding in Extended Structures. VCH, New York
[11] Gross EKU, Dobson JF, Petersilka M (1996) In: Nalewajski RF (ed) Density Functional Theory. Springer, Heidelberg
[12] Hirshfeld FL (1977) Theor Chim Acta **44**: 129
[13] Wiberg KB, Rablen PR (1993) J Comput Chem **14**: 1504